Environmental Science & Technology

pubs.acs.org/est

Article

Aerosol Iron Solubility Specification in the Global Marine Atmosphere with Machine Learning

Jinhui Shi,*,‖ Yang Guan,‖ Huiwang Gao, Xiaohong Yao, Renzheng Wang, and Daizhou Zhang*

Cite This: *Environ. Sci. Technol.* 2022, 56, 16453−16461

Read Online

ACCESS | Metrics & More | Article Recommendations | Supporting Information

ABSTRACT: Aerosol iron (Fe) solubility is a key factor for the assessment of atmospheric nutrients input to the ocean but poorly specified in models because the mechanism of determining the solubility is unclear. We develop a deep learning model to project the solubility based on the data that we observed in a coastal city of China. The model has five variables: the size range of particles, relative humidity, and the ratios of sulfate, nitrate and oxalate to total Fe (TFe) contents in aerosol particles. Results show excellent statistical agreements with the solubility in the literature over most worldwide seas and margin areas with the Pearson correlation coefficients (r) as large as 0.73−0.97. The exception is the Atlantic Ocean, where good agreement is obtained with the model trained using local data (r: 0.34−0.66). The model further uncovers that the ratio of oxalate/TFe is the most important variable influencing the solubility. These results indicate the feasibility of treating the solubility as a function of the six factors in deep learning models with careful training and validation. Our model and projected solubility provide innovative options for better quantification of air-to-sea input of aerosol soluble Fe in observational and model studies in the global marine atmosphere.

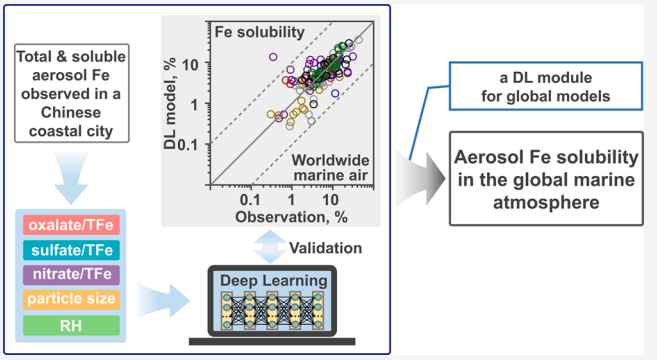

KEYWORDS: *total and soluble aerosol Fe, size-segregated particles, acidic components, relative humidity, deep learning model, worldwide ocean air*

INTRODUCTION

The input of soluble iron (Fe), recognized as bioavailable Fe, via the deposition of atmospheric aerosol particles into the ocean fertilizes the marine ecosystem, consequently enhancing the carbon export efficiency of the marine biological pump from the surface to the deep ocean and improving atmospheric CO_2 uptake in the ocean.[1,2] To better describe air−sea interactions in climate models, accurate simulation or reconstruction of soluble Fe content in aerosol particles is essential. However, even models with deliberate considerations of current understandings of the occurrence of soluble Fe in aerosol particles are unable to appropriately reproduce the observed aerosol Fe solubility on the global scale.[3−5]

Soluble Fe in aerosols originates from sources of primary particles, such as desert dust and pyrogenic particles, and/or is produced via chemical conversions of insoluble Fe in particles in the air.[6−9] Following recent progress in understanding particle emissions and processes associated with aerosol soluble Fe formation, numerical models are gradually updated and improved to match and reproduce the observed Fe solubility on a global average.[3,4] However, this improved match is partly due to the offset of an overestimation over some regions by an underestimation over other regions. For example, the improved Integrated Massively Parallel Atmospheric Chemical Transport (IMPACT) model overestimated the solubility over the Arabian Sea by a factor of more than 10, while it underestimated the solubility over the Southern Ocean by a factor of about 9.[4] Such discrepancies between model simulation and field observation indicate inadequate schemes of aerosol soluble Fe occurrence in current models.[5] It is difficult to minimize the discrepancies without a better understanding of the linkage of the primary emissions and chemical conversions with aerosol soluble Fe. Unfortunately, factors influencing aerosol soluble Fe formation usually work nonlinearly with complex overlapping, which limits emerging discoveries, i.e., the identification of the factors determining the contents of soluble Fe in aerosol particles and the assessment of the roles of each factor.

Deep learning neural network (DLNN) models based on artificial intelligence machine learning are used as increasingly powerful tools for predicting or simulating various complex

Received: July 22, 2022
Revised: October 19, 2022
Accepted: October 20, 2022
Published: October 31, 2022

phenomena. This approach exhibits great flexibility in learning and generalization to capture intricate patterns in collected datasets without requiring a comprehensive understanding of the mechanisms linking input variables with predictor variables.[10] DLNN models have demonstrated their outstanding performance for various challenging Earth science applications.[11−13]

In this study, we challenge the prediction of aerosol Fe solubility observed in the global marine atmosphere using a DLNN model that we construct, train and validate, and describe the factors determining aerosol Fe solubility upon the model performance in comparison with literature data and traditional model simulation. As shown below, our model specifies factors determining the solubility and shows good skills in reproducing Fe solubility in aerosol particles observed in worldwide marine air. Incorporating the DLNN model as a module or directly the model projected solubility into global models is expected to largely improve the accuracy of predicting air-to-sea soluble Fe input on local, regional, and global scales.

MATERIALS AND METHODS

Data for Model Construction. Observational data from 11 sets of size-segregated aerosol samples were used to train and validate the DLNN model. The samples were collected with 9-stage cascade impactors (particle size ranges: ≤0.43, 0.43−0.65, 0.65−1.1, 1.1−2.1, 2.1−3.3, 3.3−4.7, 4.7−7.0, 7.0−11, and >11 μm) on the Laoshan campus of Ocean University of China (36°09′N, 120°29′E), which is approximately 7 km from the coast of the Yellow Sea, China. Acid-washed Whatman 41 fiber filters were used for trace metal analysis, and Pallflex fiber-film T60A20 filters were used for water-soluble ion analysis. Operational filter blanks were also collected. After a series of pretreatments, the contents of Fe and other metals (e.g., Al, Mn, Ba, Zn, and Pb) in the samples and blank filters were quantified using an inductively coupled plasma mass spectrometer (Agilent 7500c ICP-MS). Water-soluble ions including sulfate, nitrate, and oxalate in the samples were analyzed using an ion chromatography instrument (Dionex ICS-3000). Details of the sample treatment and analytical procedures and accuracy are described by Shi et al.[14,15]

During sample collection, we encountered fog, haze, and rain besides clear weather. With the meteorological records published by the China Meteorological Administration and our records of visibility during the collection of each sample, the samples were categorized into four groups: fog samples, fog and haze mixed samples, clear-day samples, and other samples (Table S1). If fog occurred more than 6 h in the period of a sample collection and there was no rain or haze during the collection, the sample was classified as a fog sample. In cases when both fog and haze occurred more than 6 h during the period of sample collection, the sample was categorized as a fog and haze sample. In cases when no fog and haze occurred or the duration of their occurrence was less than 6 h, the average visibility was larger than 10 km, and the relative humidity (RH) was smaller than 70% in the periods of sample collection, the samples were classified as clear-day samples. The remaining samples, i.e., those obtained during fog or haze and over more than 6 h while the average visibility was less than 10 km or RH was smaller than 70% or those obtained under precipitation for the duration of sample collection, were classified as other samples. Upon classification, we obtained two sets of fog samples, two sets of fog and haze samples, three sets of clear samples, and four sets of other samples in our field observations.

Model Input Variable Selection. Only a small number of data are available for training and validating the DLNN model due to the scarcity of Fe solubility data in size-segregated aerosol particles. We attempted to select input variables suitable for representing factors that may govern and influence Fe solubility, which was crucial for model construction and simulation accuracy. We also tried to minimize the number of input variables in consideration of limited observation data and probable model overfitting.

Soluble Fe in aerosol particles originates from particle sources and the conversion of insoluble Fe to soluble Fe in the atmosphere.[4,5] The former is determined by the apportionments of the two major sources of natural mineral dust and pyrogenic source emissions. Natural mineral dust has a low fraction of soluble Fe, whereas pyrogenic particles emitted by coal combustion, ships, metal smelting industry, and biomass burning have a high fraction of soluble Fe.[16−19] The conversion includes the proton-promoted dissolution of insoluble Fe coinciding with sulfate and nitrate formation and ligand-promoted dissolution with oxalate formation when particles are suspended in air.[20−23] In the global atmosphere, approximately 95% of total aerosol Fe is from natural mineral dust and the rest is mainly from anthropogenic emissions.[24−27] The emission of anthropogenic Fe-containing particles is usually accompanied by gaseous pollutants such as sulfur dioxide (SO_2), nitrogen oxides (NO_x), and volatile organic compounds, which are precursor gases for sulfate, nitrate, and oxalic acid. The formation of acidic species associated with these precursor gasses in particles is the major cause driving the conversion of insoluble Fe to soluble Fe.[5,22] The production rate of soluble Fe in the aerosol acidification process is also dependent on ambient RH because the conversion process is more efficient under humid conditions.[14,28] Moreover, the content of soluble Fe in aerosol particles is closely related to aerosol particle size.[28,29]

Based on these findings, the molar ratios of sulfate, nitrate, and oxalate to total Fe (TFe) in aerosol samples, the size range of particles, and the ambient RH were selected as input variables for the DLNN model. We adopted the ratios of sulfate/TFe, nitrate/TFe, and oxalate/TFe rather than the respective mole concentration of these components because the ratios better reflect the impact of aerosol acidification and oxalate complexation on the conversion of aerosol insoluble Fe and indirectly represent the apportionments of anthropogenic particles and natural mineral dust in aerosol samples[14,30] while reducing the number of required input variables. Moreover, the parameters involving sulfate and nitrate also reflect the influence of pyrogenic sources. The reason is that a large fraction of the salts in the atmosphere are formed via the conversion of their precursor gases of sulfur dioxide and nitrogen oxides, which are mainly emitted from biomass burning and fossil fuel combustion in East Asia.[31,32]

DLNN Model Construction. The DLNN model is a multilayer perceptron neural network involving multiple layers acting as the building blocks of the network. Its advantage over other statistical techniques is the good ability to detect complex nonlinear patterns between controlling and predictor variables.[10] In this study, the DLNN model was constructed to predict aerosol Fe solubility. Five controlling variables, including six factors, such as sulfate, nitrate, oxalate, and

https://doi.org/10.1021/acs.est.2c05266
Environ. Sci. Technol. 2022, 56, 16453−16461

total Fe (TFe) in aerosol samples, aerosol particle size, and the RH of ambient air when samples were collected were input into the model for training, validation, and prediction. The input data were normalized with a zero-mean (z-score). Mini-batch Gradient Descent was used to optimize the DLNN model.[33] The epoch of the model was 500, and the batch size of each epoch was 32. In addition, Adaptive Moment Estimation (Adam) was used for gradient optimization,[33] and mean squared error was used as the loss function to investigate the fitting accuracy.

We recently revealed that fog could significantly promote the dissolution of aerosol insoluble Fe and enhanced Fe solubility by the feedback between aerosol acidification and Fe catalysis.[14] Proper inclusion of the influence of fog in the model is essential. The observation datasets at Qingdao were divided into four categories according to the weather and air pollution conditions, which were categorized as fog, fog and haze, clear, and other conditions. Input data to train the model were seven randomly selected sets from each category, but at least one set was left in the category for the model validation, which ensured the coverage of the model training and validation to weather conditions and air pollution situations. Therefore, model training involved the influence of fog on Fe solubility.

The DLNN model structure consists of one input layer, several hidden layers, and one output layer. We tested DLNN configurations with multiple assemblies of input variables and a different number of hidden layers and neurons to optimize the DLNN model. The performance of the model was assessed with four indices, including the Pearson correlation coefficient (r), root mean square error (RMSE), normalized mean deviation (NMB), and normalized mean error (NME). Finally, the optimized DLNN model consists of one input layer with five neurons (sulfate/TFe, nitrate/TFe, oxalate/TFe, aerosol particle size, and RH), five hidden layers with 200 neurons in each layer, and one output layer with 1 neuron (Fe solubility). The activation functions of each neuron in both hidden and output layers use the rectified linear unit (ReLU). The detailed configuration of the DLNN model is shown in Figure S1. The learning experiments were run using AIforScience produced by Beijing Diji Tech, which is a platform to accelerate implementing and explaining deep learning algorithms.

The reproduced Fe solubility by the model after training strongly matches solubility for training (Figure S2a). The r, RMSE, NMB, and NME between the reproduced solubility and the observed solubility were 0.99, 1.0, 0.49%, and 10.1%, respectively, demonstrating the high reliability of the model training. The effectiveness of the trained model was verified with the data from the remaining four sets of samples. The model predicted the solubility with reasonably high accuracy to the observed solubility in each case, despite differences in weather conditions and air pollution situations (Figure S2b). The r, RMSE, NMB, and NME between the simulated and observed solubility were 0.97, 2.6, 15.9%, and 25.2%, respectively, testifying the excellent capability of the model to predict aerosol Fe solubility at Qingdao.

Sensitivity Analysis. The DLNN sensitivity analysis was performed to further explore the mechanisms underlying the complex process of Fe solubilization governed by the input variables. We adopted the SHapley Additive exPlanations (SHAP) value approach to examine the potential contributions of these variables to the solubility. This approach was developed by Lundberg and Lee[34] to examine the potential contributions of the controlling variables to Fe solubility. The SHAP value describes the contribution from every feature of the input variables to the predictor variables and is defined by

$$\varphi_i = \sum_{S \subseteq N \setminus \{i\}} \frac{|S|!(N - |S| - 1)!}{|N|!} (f(S \cup \{i\}) - f(S))$$

where N represents the total number of input variables, and S represents subsets of N without feature i. The effect of input variables is derived from the cooperation of all features. The effect of feature i is obtained by subtracting $f(S)$ from $f(S \cup \{i\})$. The SHAP value φ_i involves all processes regarding the feature i. A positive SHAP value indicates an increasing effect of the input variables on the prediction variable, a negative SHAP value indicates a decreasing effect, and an absolute SHAP value indicates the net effect.

Literature Data for Global Testing. All currently available literature data on the Fe solubility in size-segregated aerosol samples collected in marine and coastal areas worldwide were applied in this study.[35−40] The concentration and solubility of Fe, the acid species concentrations (sulfate, nitrate, and oxalate) in the aerosol samples, aerosol particle size, and the ambient RH during the sample collection were extracted from the literature to establish a testing dataset for the model. In most cases, the literature reported only the concentration and solubility of Fe in aerosols without providing corresponding data, such as acidic species and RH. For those cases, we compensated for the lack of data using data obtained from other sources. For the aerosol samples in Hiroshima, Japan,[39] the oxalate concentration was estimated with the sulfate concentration at Hiroshima and the ratio of oxalate to sulfate at Tsukuba, Japan,[41] and the RH was from the historical weather records (https://rp5.ru/). For data from the Southern Ocean, the concentration and solubility of Fe and the ambient RH were from Gao et al.[37] and the corresponding acid species concentrations from Xu et al.[42] For the data over the Arctic Ocean[38] and the Atlantic Ocean,[35,36] RH was from the weather database (https://www.ready.noaa.gov/index.php). In addition, in the case of the US East Coast,[40] the Fe solubility was determined with a hydrochloric acid solution of pH 1.0 as the leaching solution, which is very different from neutral pure water as the leaching solution in most cases. Chang et al.[43] reported that the Fe solubility in HCl solution (pH = 2.0) was about fivefold of that in pure water. Therefore, we used one-fifth of the reported aerosol Fe solubility data from the US East Coast in the simulation to allow the comparability with the solubility in pure water.

In total, we got 163 aerosol samples (26 sets) that met the required parameters of the model testing, of which 14 samples (2 sets) at coastal areas of Japan, 30 samples (3 sets) on the US East Coast, 10 samples (1 set) at the Southern Ocean, 16 samples (8 sets) at the Arctic Ocean, 27 samples (4 sets) at the Tropical Atlantic Ocean, and 66 samples (8 sets) at the North Atlantic Ocean. The detailed information on each sample is shown in Table S2.

RESULTS AND DISCUSSION

Application to Marine Air Globally. From the published literature, we acquired 163 datasets of aerosol samples that met the requirements for the input factors for the constructed DLNN model.[35−40] The samples were collected in global marine and coastal areas (Materials and Methods). We used the six factors in each dataset to predict Fe solubility in the

https://doi.org/10.1021/acs.est.2c05266
Environ. Sci. Technol. 2022, 56, 16453−16461

relevant aerosol sample with the DLNN model and compared the model results with the observed solubility. Results show a very good agreement between the model and observations at the coastal areas of Japan, the US East Coast, the Southern Ocean, and the Arctic Ocean (Figure 1a–d). The *r*, RMSE, NMB, and NME were 0.73–0.84, 2.3–3.8, −4.8–15.7%, and 27.1–41.5%, respectively (Table S3). However, the prediction did not match well with observations in the Atlantic Ocean (Figure 1e,f). In particular, the *r* was −0.08 and RMSE was 11.3 for the North Atlantic. This discrepancy is likely attributable to the low concentration of acid components and soluble Fe in some samples. Of the 66 data points observed in the North Atlantic, 55 for sulfate and 63 for nitrate were below the detection limit.[36] Of the 27 data points for aerosol soluble Fe observed in the air over the Tropical Atlantic Ocean, the concentration for 11 data points was below the detection limit.[35] Assigning detection limits to the input values of the factors prevented the DLNN model from developing good links between variables and Fe solubility, which can cause significant prediction uncertainties.

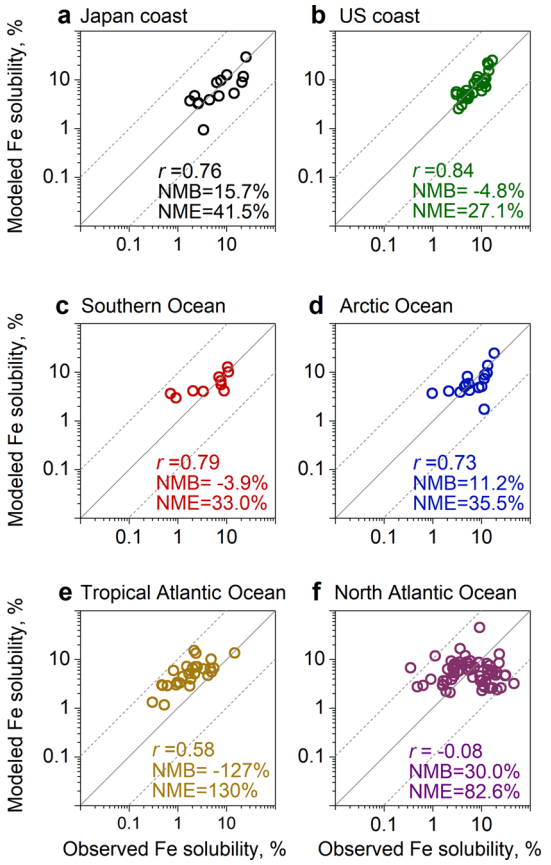

Figure 1. (a–f) Comparison of DLNN model-simulated aerosol Fe solubility in the global marine air with observations reported in the literature.

To improve the simulation results for the Atlantic Ocean, we retrained the model with about 60% of data obtained in the examination region and simulated the solubility in the rest datasets. Results show that the prediction accuracy of the retrained model was largely improved (Figure 2). The *r* and RMSE were upgraded to 0.34 and 7.9 at the North Atlantic and 0.66 and 2.9 at the Tropical Atlantic (Table S4). These results indicate that our constructed DLNN model can

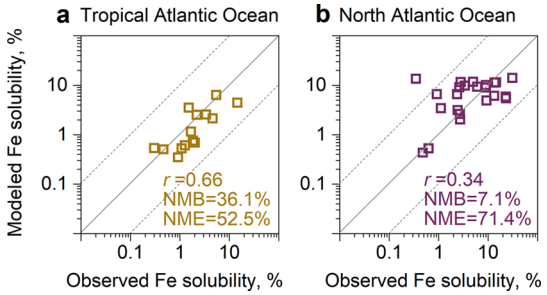

Figure 2. (a,b) Similar to Figure 1e,f, but the DLNN model was trained with part data in the Atlantic Ocean.

effectively predict aerosol Fe solubility in the global marine atmosphere. Trained with data from the coastal area of China, the simulation results matched well with observations in the global marine atmosphere excluding that of the Atlantic Ocean, where the model required training with local data.

Model Performance Evaluation. To verify the robustness of the constructed DLNN model, we compared the model performance with the IMPACT model by Ito et al.,[4,5] which is the latest traditional model focusing on soluble Fe in aerosol particles in the global atmosphere. We limited the comparison to the coastal areas of China, Japan, the United States, the Southern Ocean, the Tropical Atlantic Ocean, and the North Atlantic Ocean where data on Fe solubility in size-segregated aerosols are available.[35−40] The comparison results are shown in Figure 3 and Table S3. The Fe solubility simulated by the DLNN model matches field observations much better than the results of the IMPACT model simulation. Specifically, the RMSE is lower in the Southern Ocean than the IMPACT model by a factor of about 7 and the NME by a factor of about 3. Our DLNN model successfully reproduced the high Fe solubility observed over the Southern Ocean, which could be attributable to the inclusion of fog effects and pyrogenic Fe contributions. Pyrogenic particles with their high initial Fe solubility are potentially important contributors in the Southern Ocean,[44,45] and fog, a frequent phenomenon in the Southern Ocean,[46] can significantly increase aerosol Fe solubility.[14]

The DLNN model trained with data at the coastal China seas failed to reproduce the observed Fe solubility only in the Atlantic Ocean air, although its results are closer to the observation than the IMPACT model (Figure 3e,f). This mismatch indicates that there are other factors besides the five input variables in the DLNN model that can make the production of aerosol soluble Fe largely different between the Atlantic Ocean and other areas, or the production in the Atlantic Ocean is governed by the examined five variables but with the working mechanism somewhat different. One candidate factor is the distinctive mineralogical characteristic of mineral dust.[47] The dust particles in the coastal areas of China are mainly from the deserts in the Asian continent and rich in goethite, and the dust particles over the Atlantic Ocean are usually from the deserts in northern Africa and rich in hematite.[48,49] The Fe solubility of hematite is higher than that of goethite.[50] The DLNN model trained with the data observed in the Atlantic Ocean reproduces solubility much better than the IMPACT model (Figure 4, Table S4), although the obtained results are not yet as accurate as predictions in other regions. The production of aerosol soluble Fe over the Atlantic Ocean can thus be described by the DLNN model

https://doi.org/10.1021/acs.est.2c05266
Environ. Sci. Technol. 2022, 56, 16453−16461

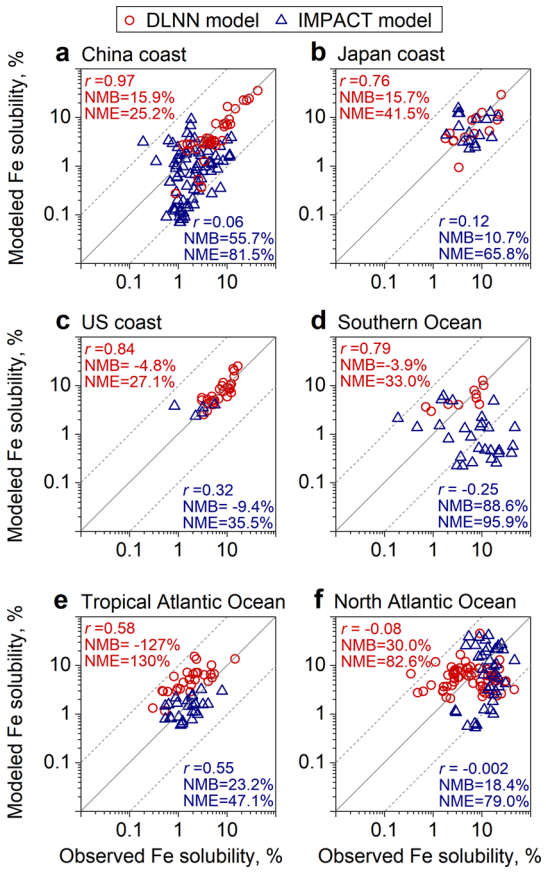

Figure 3. (a–f) Comparison of simulated aerosol Fe solubility by the present DLNN model and the IMPACT model[4,5,14] versus observations in the global marine air. The solid line in each panel shows the 1:1 ratio, and the two dotted lines represent ±10% deviation between the observed and simulated values.

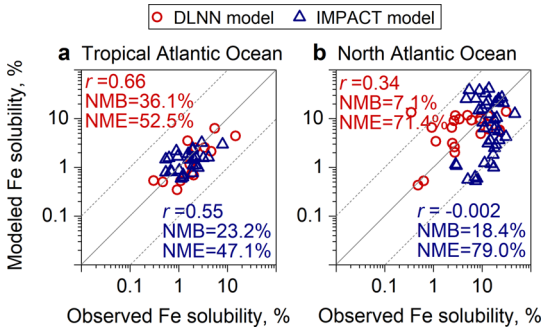

Figure 4. (a,b) Similar to Figure 3e,f, but the DLNN model was trained with part data in the Atlantic Ocean.

largely with the five variables but only with the training using local data. In addition, the concentration of sulfate, nitrate, and soluble Fe in the aerosol particles observed in the North Atlantic was very low, which led to uncertainties in the simulation. All of these can be improved by adding variables to the model and with more observation data for model training and validation in the future, particularly for aerosol particles over the Atlantic Ocean.

Significance of Oxalate, Sulfate, and Nitrate. The DLNN model reasonably predicted the Fe solubility with the five variables. Here, we investigated the dependence of Fe solubility on each variable using sensitivity analysis. Among the five input variables, the molar ratio of oxalate/TFe plays the most significant role in regulating Fe solubility and promoting Fe dissolution, which is described using the index SHAP; its significance is as great as 4-fold that of sulfate/TFe and 11-fold that of nitrate/TFe (Figure 5a). The ratio of oxalate/TFe has a

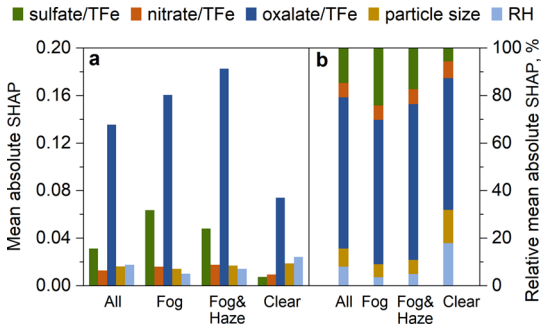

Figure 5. SHAP of the input variables under different weather conditions. (a) Mean absolute SHAP values; (b) relative contribution to Fe solubility.

threshold of 0.7 nmol/nmol (Figure S3), above which the promotion is obvious, a phenomenon occurring frequently in the marine atmosphere in which the content of total aerosol Fe is usually very low.[16]

Laboratory experiments have also shown an increased Fe dissolution due to oxalate compared to sulfate-promoted dissolution, but the concentration of oxalic acid must be sufficient to overcome the competition of soluble Fe in particles so that the excess oxalate would efficiently enhance insoluble Fe dissolution.[20] Model simulations with oxalate-promoted Fe dissolution involved improved the accuracy of simulated Fe solubility,[24,51,52] e.g., from 32 to 86% on average, but very large discrepancies remained for individual cases.[3] In the present study, the oxalate/TFe contributes approximately 60% of Fe solubility (Figure 5b). The contribution of sulfate/TFe is approximately 20% under fog and fog and haze conditions and 10% under clear weather conditions, and the contribution of nitrate/TFe is stable at approximately 10%.

Sulfate/TFe and oxalate/TFe have a coordination effect after the latter exceeds its threshold, while no such effect is observed between nitrate/TFe and oxalate/TFe (Figure 6a). Chen and Grassian[20] reported that the aerosol Fe solubility in a sulfuric acid solution of pH 2 was enlarged approximately threefold by adding 2.0 mM oxalic acid. However, adding 0.1 mM oxalic acid did not cause a considerable change in solubility. In polluted air, the acidification of mineral particles associated with sulfate and nitrate is initially triggered by nitrate formation, which enables particles to absorb water vapor at low RH and thus accelerates the formation of the two salts after the particles form an aqueous layer.[53−55] In addition, nitric acid suppresses Fe(II) formation under low pH conditions.[56] Therefore, insoluble Fe dissolution associated with nitrate formation likely occurs only in the early stage of aerosol acidification when nitrate formation is predominant, the consequence of which could be the stable relative contribution of nitrate/TFe and the lack of a coordination effect between nitric acid and oxalic acid (Figure 6b).

Significance of Particle Size and Air Relative Humidity. The sizes of aerosol particles and the RH of ambient air together account for approximately 10% of the impact of the five variables on Fe solubility in fog and fog and

https://doi.org/10.1021/acs.est.2c05266
Environ. Sci. Technol. 2022, 56, 16453−16461

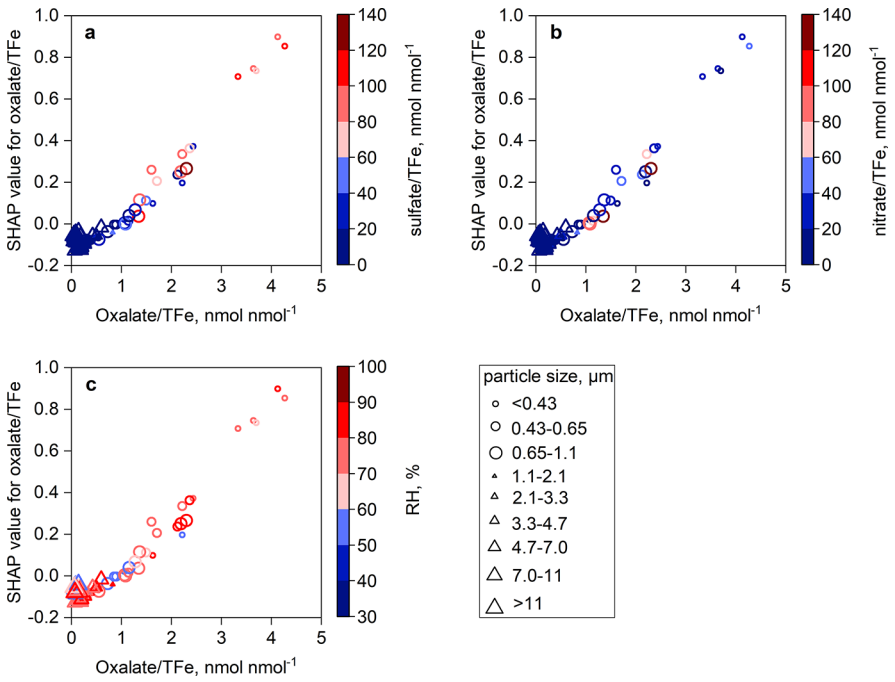

Figure 6. Relationship between oxalate/TFe and its SHAP value with particle sizes and dependence on (a) the ratio of sulfate/TFe, (b) the ratio of nitrate/TFe, and (c) RH.

haze samples, while their contribution is more than 30% in clear day samples (Figure 6c). The high RH, more than 70% in the present study, in fog and fog and haze days could make water-soluble components in the particles deliquesced and produce an aqueous layer on the particles. The above-mentioned acidification in the aqueous phase on the surface of particles would dominate the conversion of insoluble Fe to soluble Fe.[14,57] Once the aqueous layer is produced, the influence of RH variation would be small. In addition, particle size exerts significant effects on Fe solubility in the range of smaller than 1.1 μm, indicating that particle size is also a vital factor in the simulation of aerosol soluble Fe, which closely relates to Fe sources and aerosol acidification processes.[58]

With a DLNN model we constructed, the hidden functional relationships among Fe solubility with sulfate/TFe, nitrate/TFe, oxalate/TFe, particle size, and ambient RH were accurately quantified. Compared with the latest traditional models, the DLNN model approach exhibits excellent statistical agreement with data from the literature. Using data observed at the coast of China to comprise a new training dataset, the r values increased to more than 0.7 and the NME values decreased to less than 42% over studied oceans except for the Atlantic Ocean, where the mechanism responsible for the formation of soluble Fe is likely different from other oceanic areas. After retraining the DLNN model with a part of data observed in the Atlantic Ocean, the model accuracy improved to 15−60% when predicting Fe solubility in this region. All these results indicate that our DLNN model can accurately specify the aerosol Fe solubility in most global marine areas with the training using data we observed in the coastal area of China and the solubility in the areas of the Atlantic Ocean with the training using Atlantic data. Therefore, the DLNN model we constructed provides an innovative approach for simulating aerosol soluble Fe in the marine atmosphere worldwide. Its performance is much better upon validation using currently available data than the latest traditional model. Incorporating the DLNN model as a module into global models to replace traditional schemes for aerosol soluble Fe quantification is expected to largely improve the accuracy of predicting the air-to-sea input of bioavailable Fe on the global scale. Before similar models can be encoded into climate models, a dataset of the solubility projected by our DLNN model with the six factors in the ranges of actual atmosphere worldwide (Data S1) is an alternate option for numerical models to quantitatively assess the global air-to-sea input of aerosol soluble Fe.

■ ASSOCIATED CONTENT

Supporting Information

The Supporting Information is available free of charge at https://pubs.acs.org/doi/10.1021/acs.est.2c05266.

Additional configuration of the DLNN model; sample collection details; summary of literature data for global testing; DLNN model training and validation results; and a dataset of the solubility projected by the DLNN model with the six factors in the ranges of the actual atmosphere worldwide (PDF)

■ AUTHOR INFORMATION

Corresponding Authors

Jinhui Shi − *Key Laboratory of Marine Environmental Science and Ecology, Ocean University of China, Ministry of Education of China, Qingdao 266100, China; Laboratory for Marine Ecology and Environmental Science, Qingdao National Laboratory for Marine Science and Technology, Qingdao 266237, China;* orcid.org/0000-0002-4986-8455; Email: engroup@ouc.edu.cn

Daizhou Zhang − *Faculty of Environmental and Symbiotic Sciences, Prefectural University of Kumamoto, Kumamoto 862-8502, Japan*; Email: dzzhang@pu-kumamoto.ac.jp

https://doi.org/10.1021/acs.est.2c05266
Environ. Sci. Technol. 2022, 56, 16453−16461

Authors

Yang Guan − *Key Laboratory of Marine Environmental Science and Ecology, Ocean University of China, Ministry of Education of China, Qingdao 266100, China*

Huiwang Gao − *Key Laboratory of Marine Environmental Science and Ecology, Ocean University of China, Ministry of Education of China, Qingdao 266100, China; Laboratory for Marine Ecology and Environmental Science, Qingdao National Laboratory for Marine Science and Technology, Qingdao 266237, China*

Xiaohong Yao − *Key Laboratory of Marine Environmental Science and Ecology, Ocean University of China, Ministry of Education of China, Qingdao 266100, China; Laboratory for Marine Ecology and Environmental Science, Qingdao National Laboratory for Marine Science and Technology, Qingdao 266237, China;* orcid.org/0000-0002-2960-0793

Renzheng Wang − *Key Laboratory of Marine Environmental Science and Ecology, Ocean University of China, Ministry of Education of China, Qingdao 266100, China*

Complete contact information is available at: https://pubs.acs.org/10.1021/acs.est.2c05266

Author Contributions

‖J.S. and Y.G. contributed equally.

Author Contributions

J.S. designed the research and instructed Y.G. to conduct the analysis. J.S., Y.G., and D.Z. wrote the manuscript. J.S. and D.Z. revised the manuscript. Y.G. prepared all the figures. R.W. prepared the projected solubility dataset. H.G. and X.Y. provided useful comments. All authors contributed toward improving the manuscript.

Notes

The authors declare no competing financial interest.

The DLNN model codes, which were written based on scikit-learn in Python, are available at http://doi.org/10.6084/m9.figshare.21350706. The aerosol Fe solubility simulated by the DLNN model based on the contents of total Fe, sulfate, nitrate, and oxalate in aerosol particles, the particle size, and air relative humidity in the ranges of the actual atmosphere worldwide are available at http://doi.org/10.6084/m9.figshare.21341730.

■ ACKNOWLEDGMENTS

The authors thank Shuai Zhang for her assistance in sample collection and part of the chemical analysis. This work was supported by the National Nature Science Foundation of China (41876131; 41876125). D.Z. was partly supported by JSPS KAKENHI 21H01158.

■ REFERENCES

(1) Jickells, T. D.; An, Z. S.; Andersen, K. K.; Baker, A. R.; Bergametti, G.; Brooks, N.; Cao, J. J.; Boyd, P. W.; Duce, R. A.; Hunter, K. A.; Kawahata, H.; Kubilay, N.; Laroche, J.; Liss, P. S.; Mahowald, N.; Prospero, J. M.; Ridgwell, A. J.; Tegen, I.; Torres, R. Global iron connections between desert dust, ocean biogeochemistry, and climate. *Science* **2005**, *308*, 67−71.

(2) Hamilton, D. S.; Moore, J. K.; Arneth, A.; Bond, T. C.; Carslaw, K. S.; Hantson, S.; Ito, A.; Kaplan, J. O.; Lindsay, K.; Nieradzik, L.; Rathod, S. D.; Scanza, R. A.; Mahowald, N. M. Impact of changes to the atmospheric soluble iron deposition flux on ocean biogeochemical cycles in the anthropocene. *Global Biogeochem. Cycles* **2020**, *34*, e2019G−e6448G.

(3) Scanza, R. A.; Hamilton, D. S.; Pérez García-Pando, C.; Buck, C.; Baker, A.; Mahowald, N. M. Atmospheric processing of iron in mineral and combustion aerosols: development of an intermediate-complexity mechanism suitable for Earth system models. *Atmos. Chem. Phys.* **2018**, *18*, 14175−14196.

(4) Ito, A.; Myriokefalitakis, S.; Kanakidou, M.; Mahowald, N. M.; Scanza, R. A.; Hamilton, D. S.; Baker, A. R.; Jickells, T.; Sarin, M.; Bikkina, S.; Gao, Y.; Shelley, R. U.; Buck, C. S.; Landing, W. M.; Bowie, A. R.; Perron, M. M. G.; Guieu, C.; Meskhidze, N.; Johnson, M. S.; Feng, Y.; Kok, J. F.; Nenes, A.; Duce, R. A. Pyrogenic iron: The Missing link to high iron solubility in aerosols. *Sci. Adv.* **2019**, *5*, eaau7671.

(5) Ito, A.; Ye, Y.; Baldo, C.; Shi, Z. Ocean fertilization by pyrogenic aerosol iron. *npj Clim. Atmos. Sci.* **2021**, *4*, 30.

(6) Meskhidze, N.; Chameides, W. L.; Nenes, A.; Chen, G. Iron mobilization in mineral dust: Can anthropogenic SO_2 emissions affect ocean productivity? *Geophys. Res. Lett.* **2003**, *30*, 2085.

(7) Mahowald, N. M.; Baker, A. R.; Bergametti, G.; Brooks, N.; Duce, R. A.; Jickells, T. D.; Kubilay, N.; Prospero, J. M.; Tegen, I. Atmospheric global dust cycle and iron inputs to the ocean. *Global Biogeochem. Cycles* **2005**, *19*, GB4025.

(8) Ito, A.; Shi, Z. Delivery of anthropogenic bioavailable iron from mineral dust and combustion aerosols to the ocean. *Atmos. Chem. Phys.* **2016**, *16*, 85−99.

(9) Matsui, H.; Mahowald, N. M.; Moteki, N.; Hamilton, D. S.; Ohata, S.; Yoshida, A.; Koike, M.; Scanza, R. A.; Flanner, M. G. Anthropogenic combustion iron as a complex climate forcer. *Nat. Commun.* **2018**, *9*, 1593.

(10) Gardner, M. W.; Dorling, S. R. Artificial neural networks (the multilayer perceptron)-a review of applications in the atmospheric sciences. *Atmos. Environ.* **1998**, *32*, 2627−2636.

(11) Reichstein, M.; Camps-Valls, G.; Stevens, B.; Jung, M.; Denzler, J.; Carvalhais, N.; Prabhat, M. Deep learning and process understanding for data-driven Earth system science. *Nature* **2019**, *566*, 195−204.

(12) Zuo, R.; Xiong, Y.; Wang, J.; Carranza, E. J. M. Deep learning and its application in geochemical mapping. *Earth-Sci. Rev.* **2019**, *192*, 1−14.

(13) Xing, J.; Zheng, S.; Ding, D.; Kelly, J. T.; Wang, S.; Li, S.; Qin, T.; Ma, M.; Dong, Z.; Jang, C. Z.; Zhu, Y.; Zheng, H.; Ren, L.; Liu, T.; Hao, J. Deep Learning for Prediction of the Air Quality Response to Emission Changes. *Environ. Sci. Technol.* **2020**, *54*, 8589−8600.

(14) Shi, J.; Guan, Y.; Ito, A.; Gao, H.; Yao, X.; Baker, A. R.; Zhang, D. High Production of Soluble Iron Promoted by Aerosol Acidification in Fog. *Geophys. Res. Lett.* **2020**, *47*, e2019GL086124.

(15) Shi, J.; Wang, N.; Gao, H.; Baker, A. R.; Yao, X.; Zhang, D. Phosphorus solubility in aerosol particles related to particle sources and atmospheric acidification in Asian continental outflow. *Atmos. Chem. Phys.* **2019**, *19*, 847−860.

(16) Sholkovitz, E. R.; Sedwick, P. N.; Church, T. M.; Baker, A. R.; Powell, C. F. Fractional solubility of aerosol iron: Synthesis of a global-scale data set. *Geochim. Cosmochim. Acta* **2012**, *89*, 173−189.

(17) Schroth, A. W.; Crusius, J.; Sholkovitz, E. R.; Bostick, B. C. Iron solubility driven by speciation in dust sources to the ocean. *Nat. Geosci.* **2009**, *2*, 337−340.

(18) Mahowald, N. M.; Hamilton, D. S.; Mackey, K. R. M.; Moore, J. K.; Baker, A. R.; Scanza, R. A.; Zhang, Y. Aerosol trace metal leaching and impacts on marine microorganisms. *Nat. Commun.* **2018**, *9*, 2614.

(19) Tang, W.; Llort, J.; Weis, J.; Perron, M. M. G.; Basart, S.; Li, Z.; Sathyendranath, S.; Jackson, T.; Rodriguez, E. S.; Proemse, B. C.; Bowie, A. R.; Schallenberg, C.; Strutton, P. G.; Matear, R.; Cassar, N. Widespread phytoplankton blooms triggered by 2019-2020 Australian wildfires. *Nature* **2021**, *597*, 370−375.

(20) Chen, H. H.; Grassian, V. H. Iron dissolution of dust source materials during simulated acidic processing: The effect of sulfuric, acetic, and oxalic acids. *Environ. Sci. Technol.* **2013**, *47*, 10312−10321.

(21) Dall'Osto, M.; Beddows, D. C. S.; Harrison, R. M.; Onat, B. Fine iron aerosols are internally mixed with nitrate in the urban European atmosphere. *Environ. Sci. Technol.* **2016**, *50*, 4212−4220.
(22) Li, W.; Xu, L.; Liu, X.; Zhang, J.; Lin, Y.; Yao, X.; Gao, H.; Zhang, D.; Chen, J.; Wang, W.; Harrison, R. M.; Zhang, X.; Shao, L.; Fu, P.; Nenes, A.; Shi, Z. Air pollution-aerosol interactions produce more bioavailable iron for ocean ecosystems. *Sci. Adv.* **2017**, *3*, No. e1601749.
(23) Zhou, Y.; Zhang, Y.; Griffith, S.; Wu, G.; Lei, L.; Zhao, Y.; Li, M.; Zhou, Z.; Yu, J. Field Evidence of Fe-Mediated Photochemical Degradation of Oxalate and Subsequent Sulfate Formation Observed by Single Particle Mass Spectrometry. *Environ. Sci. Technol.* **2020**, *54*, 6562−6574.
(24) Myriokefalitakis, S.; Daskalakis, N.; Mihalopoulos, N.; Baker, A. R.; Nenes, A.; Kanakidou, M. Changes in dissolved iron deposition to the oceans driven by human activity: a 3-D global modelling study. *Biogeosciences* **2015**, *12*, 3973−3992.
(25) Luo, C.; Mahowald, N.; Bond, T.; Chuang, P. Y.; Artaxo, P.; Siefert, R.; Chen, Y.; Schauer, J. Combustion iron distribution and deposition. *Global Biogeochem. Cycles* **2008**, *22*, GB1012.
(26) Wang, R.; Balkanski, Y.; Boucher, O.; Bopp, L.; Chappell, A.; Ciais, P.; Hauglustaine, D.; Peñuelas, J.; Tao, S. Sources, transport and deposition of iron in the global atmosphere. *Atmos. Chem. Phys.* **2015**, *15*, 6247−6270.
(27) Rathod, S. D.; Hamilton, D. S.; Mahowald, N. M.; Klimont, Z.; Corbett, J. J.; Bond, T. C. A mineralogy-based anthropogenic combustion-iron emission inventory. *J. Geophys. Res. Atmos.* **2020**, *125*, No. e2019JD032114.
(28) Cartledge, B. T.; Marcotte, A. R.; Herckes, P.; Anbar, A. D.; Majestic, B. J. The impact of particle size, relative humidity, and sulfur dioxide on iron solubility in simulated atmospheric marine aerosols. *Environ. Sci. Technol.* **2015**, *49*, 7179−7187.
(29) Baker, A. R.; Jickells, T. D. Mineral particle size as a control on aerosol iron solubility. *Geophys. Res. Lett.* **2006**, *33*, L17608.
(30) Buck, C. S.; Landing, W. M.; Resing, J. A.; Lebon, G. T. Aerosol iron and aluminum solubility in the northwest Pacific Ocean: Results from the 2002 IOC cruise. *Geochem., Geophys., Geosyst.* **2006**, *7*, Q04M07.
(31) Fu, X.; Wang, S.; Zhao, B.; Xing, J.; Cheng, Z.; Liu, H.; Hao, J. Emission inventory of primary pollutants and chemical speciation in 2010 for the Yangtze River Delta region, China. *Atmos. Environ.* **2013**, *70*, 39−50.
(32) Hsu, S. C.; Gong, G. C.; Shiah, F. K.; Hung, C. C.; Kao, S. J.; Zhang, R.; Chen, W. N.; Chen, C. C.; Chou, C. C. K.; Lin, Y. C.; Lin, F. J.; Lin, S. H. Sources, solubility, and acid processing of aerosol iron and phosphorous over the South China Sea: East Asian dust and pollution outflows vs. Southeast Asian biomass burning. *Atmos. Chem. Phys. Discuss.* **2014**, *14*, 21433−21472.
(33) Ruder, S.*An overview of gradient descent optimization algorithms*. 2016, arXiv (Computer Science, Machine Learning), arXiv:1609.04747[cs.LG], http://arxiv.org/abs/1609.04747 (accessed February 05, 2021).
(34) Lundberg, S. M.; Lee, S. A unified approach to interpreting model predictions. *Adv. Neur. In.* **2017**, *1*, 4765−4774.
(35) Baker, A. R.; Li, M.; Chance, R. Trace metal fractional solubility in size-segregated aerosols from the tropical eastern Atlantic Ocean. *Global Biogeochem. Cycles* **2020**, *34*, No. e2019GB006510.
(36) Buck, C. S.; Landing, W. M.; Resing, J. A. Particle size and aerosol iron solubility: A high-resolution analysis of Atlantic aerosols. *Mar. Chem.* **2010**, *120*, 14−24.
(37) Gao, Y.; Xu, G.; Zhan, J.; Zhang, J.; Li, W.; Lin, Q.; Chen, L.; Lin, H. Spatial and particle size distributions of atmospheric dissolvable iron in aerosols and its input to the Southern Ocean and coastal East Antarctica. *J. Geophys. Res. Atmos.* **2013**, *118*, 12634−12648.
(38) Gao, Y.; Marsay, C. M.; Yu, S.; Fan, S.; Mukherjee, P.; Buck, C. S.; Landing, W. M. Particle-size variability of aerosol iron and impact on iron solubility and dry deposition fluxes to the Arctic Ocean. *Sci. Rep.* **2019**, *9*, 16653.
(39) Kurisu, M.; Takahashi, Y.; Iizuka, T.; Uematsu, M. Very low isotope ratio of iron in fine aerosols related to its contribution to the surface ocean. *J. Geophys. Res. Atmos.* **2016**, *121*, 11119−11136.
(40) Xia, L.; Gao, Y. Chemical composition and size distributions of coastal aerosols observed on the US East Coast. *Mar. Chem.* **2010**, *119*, 77−90.
(41) Takahashi, Y.; Furukawa, T.; Kanai, Y.; Uematsu, M.; Zheng, G.; Marcus, M. A. Seasonal changes in Fe species and soluble Fe concentration in the atmosphere in the Northwest Pacific region based on the analysis of aerosols collected in Tsukuba. *Jpn. Atmos. Chem. Phys.* **2013**, *13*, 7695−7710.
(42) Xu, G.; Gao, Y.; Lin, Q.; Li, W.; Chen, L. Characteristics of water-soluble inorganic and organic ions in aerosols over the Southern Ocean and coastal East Antarctica during austral summer. *J. Geophys. Res. Atmos.* **2013**, *118*, 13303−13318.
(43) Chang, Y.; Feng, C.; Qu, J.; Zhang, J. Soluble of metals within TSP in Shanghai. *Environ. Sci.* **2015**, *36*, 1164−1172.
(44) Ito, A.; Perron, M. M. G.; Proemse, B. C.; Strzelec, M.; Gault-Ringold, M.; Boyd, P. W.; Bowie, A. R. Evaluation of aerosol iron solubility over Australian coastal regions based on inverse modeling: implications of bushfires on bioaccessible iron concentrations in the Southern Hemisphere. *Prog. Earth Planet. Sci.* **2020**, *7*, 42.
(45) Liu, M.; Matsui, H.; Hamilton, D. S.; Lamb, K. D.; Rathod, S. D.; Schwarz, J. P.; Mahowald, N. M. The underappreciated role of anthropogenic sources in atmospheric soluble iron flux to the Southern Ocean. *npj Clim. Atmos. Sci.* **2022**, *5*, 28.
(46) Yang, Q.; Zhang, L.; Xue, Z.; Xu, C. Analyses of sea fog at Great Wall Station, Antarctica. *Chin. J. Polar Res.* **2007**, *19*, 111−120.
(47) Hamilton, D. S.; Scanza, R. A.; Feng, Y.; Guinness, J.; Kok, J. F.; Li, L.; Liu, X.; Rathod, S. D.; Wan, J. S.; Wu, M.; Mahowald, N. M. Improved methodologies for Earth system modelling of atmospheric soluble iron and observation comparisons using the Mechanism of Intermediate complexity for Modelling Iron (MIMI v1.0). *Geosci. Model Dev.* **2019**, *12*, 3835−3862.
(48) Arimoto, R.; Balsam, W.; Schloesslin, C. Visible spectroscopy of aerosol particles collected on filters: iron-oxide minerals. *Atmos. Environ.* **2002**, *36*, 89−96.
(49) Shen, Z. X.; Cao, J. J.; Zhang, X. Y.; Arimoto, R.; Ji, J. F.; Balsam, W. L.; Wang, Y. Q.; Zhang, R. J.; Li, X. X. Spectroscopic analysis of iron-oxide minerals in aerosol particles from northern China. *Sci. Total Environ.* **2006**, *367*, 899−907.
(50) Journet, E.; Desboeufs, K. V.; Caquineau, S.; Colin, J. L. Mineralogy as a critical factor of dust iron solubility. *Geophys. Res. Lett.* **2008**, *35*, L07805.
(51) Johnson, M. S.; Meskhidze, N. Atmospheric dissolved iron deposition to the global oceans: effects of oxalate-promoted Fe dissolution, photochemical redox cycling, and dust mineralogy. *Geosci. Model Dev.* **2013**, *6*, 1901−1947.
(52) Ito, A. Atmospheric processing of combustion aerosols as a source of bioavailable iron. *Environ. Sci. Technol. Lett.* **2015**, *2*, 70−75.
(53) Shi, Z.; Zhang, D.; Hayashi, M.; Ogata, H.; Ji, H.; Fujiie, W. Influences of sulfate and nitrate on the hygroscopic behaviour of coarse dust particles. *Atmos. Environ.* **2008**, *42*, 822−827.
(54) Zhang, Y.; Bao, F.; Li, M.; Chen, C.; Zhao, J. Nitrate-enhanced oxidation of SO_2 on mineral dust: a vital role of a proton. *Environ. Sci. Technol.* **2019**, *53*, 10139−10145.
(55) Cheng, Y.; Zheng, G.; Wei, C.; Mu, Q.; Zheng, B.; Wang, Z.; Gao, M.; Zhang, Q.; He, K.; Carmichael, G.; Pöschl, U.; Su, H. Reactive nitrogen chemistry in aerosol water as a source of sulfate during haze events in China. *Sci. Adv.* **2016**, *2*, No. e1601530.
(56) Cwiertny, D. M.; Baltrusaitis, J.; Hunter, G. J.; Laskin, A.; Scherer, M. M.; Grassian, V. H. Characterization and acid-mobilization study of iron-containing mineral dust source materials. *J. Geophys. Res. Atmos.* **2008**, *113*, D05202.
(57) Zhu, Y.; Li, W.; Lin, Q.; Yuan, Q.; Liu, L.; Zhang, J.; Zhang, Y.; Shao, L.; Niu, H.; Yang, S.; Shi, Z. Iron solubility in fine particles associated with secondary acidic aerosols in east China. *Environ. Pollut.* **2020**, *264*, No. 114769.

(58) Liu, L.; Li, W.; Lin, Q.; Wang, Y.; Zhang, J.; Zhu, Y.; Yuan, Q.; Zhou, S.; Zhang, D.; Baldo, C.; Shi, Z. Size-dependent aerosol iron solubility in an urban atmosphere. *npj Clim. Atmos. Sci.* **2022**, *5*, 53.

https://doi.org/10.1021/acs.est.2c05266
Environ. Sci. Technol. 2022, 56, 16453−16461